Anal Bioanal Chem (2012) 403:145–149
DOI 10.1007/s00216-012-5830-0

SHORT COMMUNICATION

Quantification of ligand packing density on gold nanoparticles using ICP-OES

Sherrie Elzey · De-Hao Tsai · Savelas A. Rabb · Lee L. Yu · Michael R. Winchester · Vincent A. Hackley

Received: 16 December 2011 / Revised: 30 January 2012 / Accepted: 1 February 2012 / Published online: 18 February 2012

Abstract In this study, a prototypical thiolated organic ligand, 3-mercaptopropionic acid (MPA), was conjugated on gold nanoparticles (AuNPs), and packing density was measured on an ensemble-averaged basis using inductively coupled plasma optical emission spectrometry. The effects of sample preparation, including centrifugation and digestion, as well as AuNP size and concentration, on recovery were investigated. For AuNPs with diameters of 5, 10, 30, 60, and 100 nm, calculated packing density is independent of size, averaging 7.8 nm^{-2} and ranging from 6.7 to 9.0 nm^{-2}, and is comparable to reported values for MPA and similar short-chain ligands on AuNPs. These preliminary data provide fundamental information on the advantages and limitations of ICP-based analyses of conjugated AuNP systems. Moreover, they provide necessary information for the development of more broadly applicable methods for quantifying nanoparticle–ligand conjugates of critical importance to nanomedicine applications.

Keywords Functional ligand · Gold nanoparticle · ICP-OES · Packing density · Quantitative analysis

Introduction

Attachment and release of functional ligands on/from engineered nanoparticles (ENPs) is important in the application of nanoparticle-based therapeutics. It is necessary to develop methods to characterize molecular conjugation in order to obtain information on molecular packing density and the corresponding molecular conformation of functional ligands on the surface of ENPs. Both packing density and conformation have been used as indicators of therapeutic performance [1, 2] and will be important for regulatory requirements and quality control in a clinical scenario.

Gold nanoparticles (AuNPs) have attracted a great deal of attention for biomedical applications such as diagnostics and drug delivery agents [3, 4]. In particular, thiol-functionalized AuNPs in medicinal applications have advanced to clinical trials for cancer treatment [4–6]. Despite such progress, there are significant challenges with respect to quality control of nano-therapeutic products, including quantification of surface-bound functional species [6, 7].

There is a need to develop methods applicable to prototypical ENP ensembles for quantification of ligands at concentrations relevant to drug delivery applications. Surface species are commonly characterized based on dimensional and optical responses. Elemental analysis is advantageous because it quantifies the core (ENP) and the coating (ligands) independently. Inductively coupled plasma optical emission spectrometry (ICP-OES) is well suited for such applications because it is highly sensitive to trace-level concentrations and small changes in concentration [8] and can simultaneously detect multiple elements. Hence, ICP-OES can, in principle, provide useful elemental information for surface species conjugated on AuNPs.

In this study, we used ICP-OES to quantify Au and S mass fractions and calculate the molecular packing density of thiol-functionalized AuNPs on an ensemble-averaged basis. First, AuNP recovery (R) was studied under different sample preparation conditions, particle sizes, and concentrations. Then, the sulfur and gold content of thiol-conjugated AuNPs was measured using optimized sample preparation conditions.

Electronic supplementary material The online version of this article (doi:10.1007/s00216-012-5830-0) contains supplementary material, which is available to authorized users.

S. Elzey · D.-H. Tsai · S. A. Rabb · L. L. Yu · M. R. Winchester · V. A. Hackley (✉)
National Institute of Standards and Technology, Material Measurement Laboratory,
Gaithersburg, MD 20899-8520, USA
e-mail: vince.hackley@nist.gov

Centrifugation and digestion were considered because centrifugation is necessary to separate coated particles from free ligands in the suspension, and digestion is required for accurate ICP-based analysis of certain ligands, such as DNA, that are commonly conjugated to nanoparticles for therapeutic applications [8]. The data reported herein will be useful for future studies aimed at improving product quality and batch-to-batch consistency of AuNP-based therapeutics and for further development of this and related analytical approaches.

Experimental

Materials

Commercially available gold nanoparticle colloidal suspensions (5, 10, 30, 60, and 100 nm; optical density OD=1) were purchased from Ted Pella[1] (Redding, CA) and (20 nm; OD=50) from BioAssay Works (Ijamsville, MD). Additionally, NIST gold nanoparticle reference materials (RMs) 8011 (10 nm) and 8013 (60 nm) were utilized. Reagent-grade nitric acid (70%, Sigma-Aldrich, St. Louis, MO) and hydrochloric acid (37%, Mallinckrodt Chemical, St. Louis, MO) were used to digest AuNP samples. Sulfur standard solution (NIST SRM 3154, lot no. 892205) and gold standard solution (NIST SRM 3121, lot no. 991806) were used to prepare working solutions as standards for ICP-OES calibration curves. Thiolated 3-mercaptopropionic acid (MPA, >99%, Sigma-Aldrich, St. Louis, MO) was used as a prototypical *S*-containing small organic ligand. Biological-grade (18 MΩ cm) high-purity deionized water (Aqua Solutions, Jasper, GA) was used for all sample preparation and dilutions.

Sample preparation

All samples and working standard solutions were prepared gravimetrically (i.e., on a mass fraction basis).

Unconjugated samples

Unconjugated AuNPs were used as received without purification to investigate the effects of centrifugation and digestion on *R*. Four conditions were studied: not centrifuged and not digested (NC-ND), not centrifuged and digested (NC-D), centrifuged and not digested (C-ND), and centrifuged and digested (C-D). The unconjugated AuNPs (1 mL) were centrifuged (MiniSpin Plus, Eppendorf North America, Hauppauge, NY) for one cycle (additional cycles prevented resuspension) under the following conditions: 100 and 60 nm for 5 min at 6,700×*g*, 30 nm for 15 min at 9,660×*g*, 20 nm for 40 min at 13,150×*g*, and 10 and 5 nm for 45 min at 14,100×*g*. After centrifugation, the supernatant was removed, approximately 1 mL of fresh DI water was added, and samples were sonicated using a Model 1510 bath sonicator (Branson, Danbury, CT) to resuspend the particles.

Conjugated samples

For conjugation, an MPA solution was prepared in water (600 mmol L^{-1}), and aliquots were added to 1 mL AuNP samples at approximately ×300 surface saturation [2], based on the diameter and particle concentration values of the AuNP suspensions reported by the manufacturers. Samples were sonicated for 20 s after MPA addition and allowed to equilibrate overnight. The MPA-AuNP samples underwent three cycles of centrifugation (see "Unconjugated samples") followed by removal of the supernatant and addition of approximately 1 mL of fresh DI water. Preliminary results showed that additional cycles (up to six) did not affect the calculated packing density of MPA within the range of uncertainty; therefore, quantitative removal of free ligands through centrifugation has been assumed in this work.

Digestion

For digested samples, HNO_3 and HCl (1:10) were added at an HCl volume equal to the final volume of the AuNPs collected after centrifugation (1 mL for NC samples); HNO_3 was added first, followed by HCl. The digestion procedure was originally developed and validated at NIST for the analysis of gold nanoparticle RMs. After several minutes, the digested sample presented a yellow solution due to dissolved gold, and it was diluted to a final HNO_3+HCl volume fraction of 2.5% for ICP-OES analysis. RMs 8011 (10 nm) and 8013 (60 nm) were studied under the four conditions at a final mass fraction of 1 μg g^{-1} Au. Commercially available AuNPs (20 nm) were studied under the four conditions at final mass fractions of approximately 5, 10, 25, and 50 μg g^{-1} Au, because the initial concentration was extremely high (equivalent to an OD of 50), enabling digestion to a final mass fraction of 50 μg g^{-1} Au (2.5% acid) without pre-concentration (NC-D).

ICP-OES analysis

Instrumental settings

An ICP-OES instrument (SPECTRO ARCOS, SPECTRO Analytical Instruments, Inc., Mahwah, NJ) was used to measure the mass fractions of Au and S using calibration

[1] The identification of any commercial product or trade name does not imply endorsement or recommendation by the National Institute of Standards and Technology.

curves generated from standard solutions. The operating conditions of the ICP-OES instrument are listed in Table 1.

Calculations

R is defined as the mass fraction of Au measured using ICP-OES divided by the known mass fraction of Au in the sample times 100%. The known mass fraction of Au was calculated for diluted samples based on the Au mass fraction reported in the manufacturer's specifications or in the RM Report of Investigation.

Packing density was calculated from the ratio of the mass fractions of S and Au measured simultaneously by ICP-OES. Assuming the absence of element-specific *R*, the calculated packing density is independent of the value of *R*. The mass fraction of S measured using ICP-OES was converted to the equivalent number of MPA ligands, and calculated MPA packing density (σ_{CALC}) was determined per square nanometer of surface area based on measured particle diameters (see Electronic supplementary material (ESM)). The equation for packing density is derived in the ESM.

Measurement uncertainty

Error bars shown in figures and uncertainty ranges associated with measurement values represent one standard deviation calculated from replicate (2 to 4) measurements performed under repeatability conditions.

Results and discussion

Recovery

Figure 1a compares the recoveries of RMs (10 and 60 nm) at ≈1 μg g^{-1} Au under the four specified conditions (NC-ND, NC-D, C-ND, and C-D) to determine the effect of particle size on *R*.

Table 1 Operating conditions of the ICP-OES instrument

Nebulizer	Cross-flow
Spray chamber	Glass–Scott type
Power (W)	1,400
Coolant gas (L min^{-1})	13.5
Auxiliary gas (L min^{-1})	1.2
Nebulizer gas (L min^{-1})	0.8
Viewing	Axial
Sample uptake (mL min^{-1})	1
Analyte wavelengths (nm)	Au 267.595
	S 180.731
Measurement time per replicate (s)	24

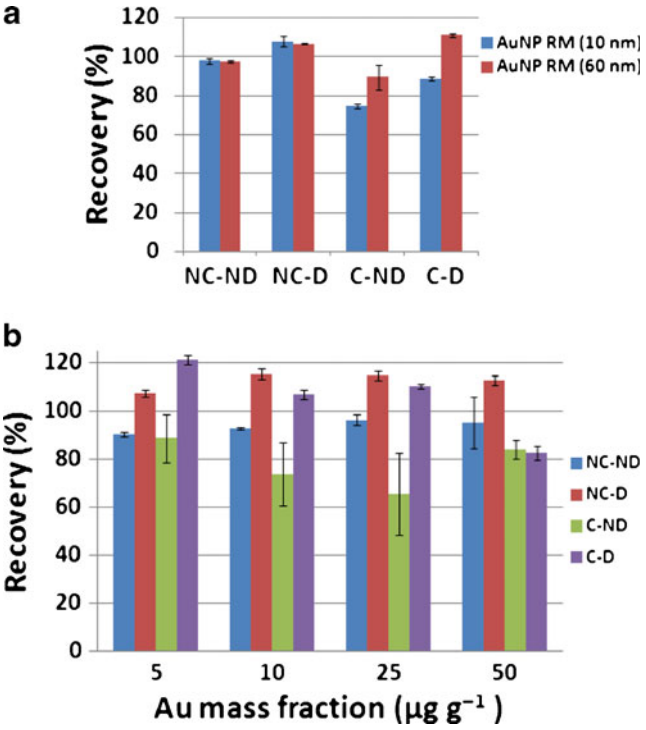

Fig. 1 Recovery of AuNPs (**a**) at ≈1 μg g^{-1} Au for RMs (10 and 60 nm) and (**b**) at various Au mass fractions for 20 nm AuNPs. *NC-ND* not centrifuged, not digested, *NC-D* not centrifuged, digested, *C-ND* centrifuged, not digested, *C-D* centrifuged, digested

For the NC-ND condition, recoveries were high for both RMs (>97%). The recoveries of the RMs increased to >100% after digestion. The additional ≈10% Au was not due to the acid, because analysis of a 1:10 HNO_3/HCl solution (2.5% acid) without AuNPs yielded only 0.03 μg g^{-1} Au (≈3%). It was not due to a memory effect because analysis of the blank between AuNP samples showed background level Au concentrations (0.02 μg g^{-1}). There was no difference in *R* for the two AuNP sizes when the samples were not centrifuged.

As expected, centrifugation resulted in lower *R* values for both samples (C-ND) because it can induce aggregation and inhibit resuspension, which may result in incomplete transport to, and atomization within, the plasma. Indeed, some of the suspensions appeared purple after centrifugation, in contrast to their initial pink/red color, indicating that aggregation occurred. Sonication and/or vortexing did not reclaim the initial color. Also, larger particles (60 nm RM) had a higher *R* than smaller particles (10 nm RM) after centrifugation; larger particles are more easily separated from the supernatant due to centrifugal force because of their higher mass. After digesting the centrifuged samples, the increase in *R* for the 10 nm RM was significant, and *R* of the 60 nm RM was the highest at >110%. The increase in *R* for centrifuged samples after digestion was likely a result of improved transport of Au into the plasma, improved atomization due to dissolution of aggregates, and/or increased removal of Au from the centrifuge tube wall.

Higher Au mass fractions correspond to higher ligand concentrations for conjugated AuNPs; thus, increased Au mass fractions may be required to detect S in large ligands and/or ligands with low surface coverage, and a range of Au mass fractions must be studied to optimize the determination of S in solution. Figure 1b shows the *R* of AuNPs at various Au mass fractions under the four conditions (NC-ND, NC-D, C-ND, and C-D). For the NC samples, the effect of Au mass fraction on *R* was minimal and, in some cases, within the range of uncertainty. The NC-ND samples were recovered at >90% at all mass fractions. The *R* of the C-ND samples decreased by approximately 20% compared with the NC-ND samples. The measurement uncertainty increased significantly for C-ND samples due to aggregation and loss of particles on the tube wall, as discussed previously. It is also possible that transport of large aggregates to the plasma through the tubing may be relatively poor. Digestion (NC-D and C-D) resulted in recoveries of >100% for nearly all samples in Fig. 1a, b. The reason for this is unclear; Au recoveries of >100% resulted only when the acid and the AuNPs were combined (i.e., not for the acid solution alone or AuNPs alone). Therefore, it is likely that an interaction between the acid species and AuNPs or Au ions caused an increase in the measured Au signal and thus an increase in *R*.

As stated above, the calculated packing density is independent of *R* when element-specific *R* effects can be neglected. As long as *R* is high enough to allow the ligand analyte (S, in this work) to be quantified, packing density can be calculated using the ratio of the measured S and Au mass fractions.

Packing density

Analysis of conjugated AuNPs was carried out without digestion (C-ND) to avoid element-specific loss during digestion and improve the likelihood that the measured ratio of the S mass fraction to the Au mass fraction is representative of the actual S/Au mass ratio in the conjugated nanoparticles. Preliminary data showed that MPA concentration was accurately detected based on S content (Fig. S2 in the ESM).

Figure 2a shows σ_{CALC} for AuNPs ranging in size from 5 to 100 nm. The calculated packing density of MPA averaged 7.8 nm^{-2}, with a range from 6.7 to 9.0 nm^{-2}. This result is comparable to reported values, which ranged from approximately 5 to 8.5 nm^{-2} for MPA on 30 nm AuNPs [7], MPA self-assembled on 50–100 nm AuNP-coated planar gold [9], and similar short-chain ligands on 30 nm AuNPs relative to planar gold [10]. Due to the small physical dimension of MPA (<1 nm) and also the insignificant difference in the surface curvature (<7°) among the different particles sizes, σ_{CALC} was independent of particle size for the size range considered in this study.

The packing density of MPA versus the Au mass fraction measured by ICP-OES is shown in Fig. 2b. These data show

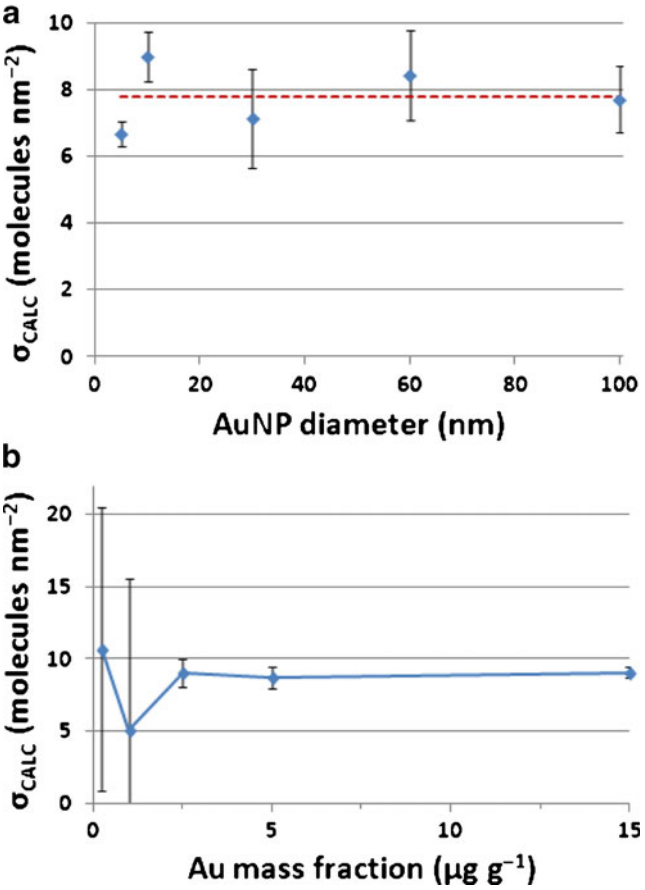

Fig. 2 Calculated packing density of MPA as a function of (**a**) AuNP size and (**b**) Au mass fraction (10 nm AuNPs). The *dashed line* in (**a**) shows the average MPA packing density

that, for MPA-coated AuNPs, Au mass fractions less than approximately 2.5 μg g^{-1} correspond to unreliable results with enormous uncertainties, including physically impossible negative packing density. Although the detection limits (as three times the standard deviation of the blank) for Au and S were 5.4 and 3.6 ng g^{-1}, respectively, unreliable results were observed for samples with S mass fractions of <20 ng g^{-1}. The measured S mass fraction decreased as Au mass fraction decreased, with S mass fractions of approximately 215, 90, 19, and 10 ng g^{-1} corresponding to Au mass fractions of approximately 15, 5, 2.5, 1, and 0.25 μg g^{-1}, respectively. Thus, to accurately quantify ligands on AuNPs using this method, the conjugated AuNPs must be sufficiently concentrated to ensure that the analyte of interest is present at a significant mass fraction.

Conclusions

ICP-OES analysis of conjugated AuNPs can be used to quantify the packing density of ligands of interest. Although *R* was affected by sample preparation, a major benefit of this method

is that the calculated packing density does not depend on R, as long as element-specific differences in R can be neglected. However, low R can be problematic, particularly for ligand detection, due to reduced analyte mass fractions in the sample.

The σ_{CALC} values were reproducible and consistent; however, we are currently developing complementary or orthogonal techniques to confirm the accuracy of the results.

These preliminary data were based on ensemble-averaged measurements, but ICP-based techniques are adaptable to hyphenation with size-separation techniques [11–13] and have the potential to be optimized for single-particle analysis [14, 15]. These data will be applied to future work focusing on other ligands of interest as well as addressing the limitations of the method, including hyphenation with size-selective techniques and improvement of detection limits using ICP-MS.

Acknowledgment This research was performed while S.E. held a National Research Council Research Associateship Award at NIST.

References

1. Dobrovolskaia MA, Patri AK, Zheng J, Clogston JD, Ayub N, Aggarwal P, Neun BW, Hall JB, McNeil SE (2009) Interaction of colloidal gold nanoparticles with human blood: effects on particle size and analysis of plasma protein binding profiles. Nanomedicine 5(2):106–117
2. Tsai D-H, Davila-Morris M, DelRio FW, Guha S, Zachariah MR, Hackley VA (2011) Quantitative determination of competitive molecular adsorption on gold nanoparticles using attenuated total reflectance–Fourier transform infrared spectroscopy. Langmuir 27 (15):9302–9313. doi:10.1021/la2005425
3. Baptista P, Pereira E, Eaton P, Doria G, Miranda A, Gomes I, Quaresma P, Franco R (2008) Gold nanoparticles for the development of clinical diagnosis methods. Anal Bioanal Chem 391 (3):943–950. doi:10.1007/s00216-007-1768-z
4. Paciotti GF, Myer L, Weinreich D, Goia D, Pavel N, McLaughlin RE, Tamarkin L (2004) Colloidal gold: a novel nanoparticle vector for tumor directed drug delivery. Drug Deliv 11(3):169–183. doi: doi:10.1080/10717540490433895
5. Smith RA, Baglioni C (1989) Multimeric structure of the tumor necrosis factor receptor of HeLa cells. J Biol Chem 264(25):14646–14652
6. Eck W, Craig G, Sigdel A, Ritter G, Old LJ, Tang L, Brennan MF, Allen PJ, Mason MD (2008) PEGylated gold nanoparticles conjugated to monoclonal F19 antibodies as targeted labeling agents for human pancreatic carcinoma tissue. ACS Nano 2(11):2263–2272. doi:10.1021/nn800429d
7. Tsai D-H, DelRio FW, MacCuspie RI, Cho TJ, Zachariah MR, Hackley VA (2010) Competitive adsorption of thiolated polyethylene glycol and mercaptopropionic acid on gold nanoparticles measured by physical characterization methods. Langmuir 26 (12):10325–10333. doi:10.1021/la100484a
8. Brennan RG, Rabb SA, Holden MJ, Winchester MR, Turk GC (2009) Potential primary measurement tool for the quantification of DNA. Anal Chem 81(9):3414–3420. doi:10.1021/ac802688x
9. El-Deab MS, Okajima T, Ohsaka T (2006) Fabrication of phase-separated multicomponent self-assembled monolayers at gold nanoparticles electrodeposited on glassy carbon electrodes. J Electrochem Soc 153(12):E201–E206
10. Tsai DH, Zangmeister RA, Pease Iii LF, Tarlov MJ, Zachariah MR (2008) Gas-phase ion-mobility characterization of SAM-functionalized Au nanoparticles. Langmuir 24(16):8483–8490. doi:10.1021/la7024846
11. Gautier E, Roberti M, Gettar R, Jiménez Rebagliati R, Batistoni D (2007) Assessment of chemical purity of 10B-enriched p-boronophenylalanine by high-performance liquid chromatography coupled on-line with inductively coupled plasma optical emission spectrometry. Anal Bioanal Chem 388(2):499–503. doi:10.1007/s00216-007-1205-3
12. Myojo T, Takaya M, Ono-Ogasawara M (2002) DMA as a gas converter from aerosol to "argonsol" for real-time chemical analysis using ICP-MS. Aerosol Sci Technol 36(1):76–83. doi:10.1080/027868202753339096
13. Lespes G, Gigault J (2011) Hyphenated analytical techniques for multidimensional characterisation of submicron particles: a review. Anal Chim Acta 692(1–2):26–41. doi:10.1016/j.aca.2011.02.052
14. Laborda F, Jimenez-Lamana J, Bolea E, Castillo JR (2011) Selective identification, characterization and determination of dissolved silver(i) and silver nanoparticles based on single particle detection by inductively coupled plasma mass spectrometry. J Anal At Spectrom 26(7):1362–1371
15. Gschwind S, Flamigni L, Koch J, Borovinskaya O, Groh S, Niemax K, Gunther D (2011) Capabilities of inductively coupled plasma mass spectrometry for the detection of nanoparticles carried by monodisperse microdroplets. J Anal At Spectrom 26(6):1166–1174